PAPER • **OPEN ACCESS**

Design, Wind Tunnel Tests, Normative and Theoretical Approaches of the ARC MAJEUR Subject to Vortex Shedding

To cite this article: A Palm *et al* 2024 *J. Phys.: Conf. Ser.* **2647** 242002

Journal of Physics: Conference Series **2647** (2024) 242002 doi:10.1088/1742-6596/2647/24/242002

Design, Wind Tunnel Tests, Normative and Theoretical Approaches of the ARC MAJEUR Subject to Vortex Shedding

A Palm[1], Y Duchêne[1], V de Ville de Goyet[1], V Denoël[2] and, T Andrianne[3]

[1] Bureau Greisch, Allée des Noisetiers 25,4031 Liège, Belgium
[2] Structural & Stochastic Dynamics, ULiege, Quartier Polytech 1, Allée de la Découverte 9,4000 Liège Belgium
[3] Wind Tunnel Laboratory, ULiege, Quartier Polytech 1, Allée de la Découverte 13D, 4000 Liège, Belgium

apalm@greich.com, yduchene@greisch.com, vdeville@greisch.com, v.denoel@uliege.be, T.Andrianne@uliege.be

Abstract. The monumental work of art by Bernar Venet, called 'Arc Majeur' wraps the Belgian motorway E411 at Lavaux-Ste-Anne, offering drivers an unmissable landmark in the landscape. This sculpture is a curved steel structure with a height of 60 meters and a 2.25 meters square section. Due to its slenderness, lightness and low vibration frequencies, the structure is very sensitive to wind excitations and mainly to vortex induced vibrations (VIV). After the presentation of the design and the main properties of the structure, the paper presents two approaches to estimate VIV amplitudes. The first one details the mathematical models of VIV included in the Eurocode and several theoretical approaches. The second approach compares the mathematical models to the results of experiments conducted in the wind tunnel facility of the University of Liège. The influence of several parameters is investigated. The experiments revealed lower VIV amplitudes than the theoretical approaches. As the Arc Majeur cannot withstand the fatigue induced by the VIV, it is mitigated by increasing the damping ratio by adding a tuned mass damper (TMD) at the top. Due to the vital importance of its operation, an online processing is developed to verify that the damper operates as intended.

1. Introduction

Imagined in the 1980s by French artist Bernar Venet, the "Arc Majeur" (Figure 1) was finally erected in Wallonia (Belgium) after numerous attempts by the artist to place his work in France. Its construction is financed by the John Cockerill Foundation and was completed in 2019.

The arc is not a continuous circular arch but a two-curvilinear-segment arc. The main arc (longest one) culminates 60 m above the motorway with a total mass of 140 tons. Together with the small arc, 20 m high and 40 tons, placed at the opposite side of the road, the ensemble frames the roadway at kilometer 99 on the E411 motorway near Lavaux-Sainte-Anne (Belgium).

The square section of the arcs is likely to produce vortex induced vibrations (VIV) in the direction perpendicular to the wind, for wind speeds of about 15-16 m/s [1, 2]. The first two natural frequencies of vibration of the main arc are close to 0.9 Hz.

Figure 1. The “Arc Majeur” during erection

Two approaches for the modelling of the vortex induced vibrations are presented. The first one details several mathematical models of VIV: the 2 models of the EN1991-1-4 [1, 2], a harmonic forcing model, the Vickery and Clark spectral model with and without tuned mass damper (TMD) and finally, the wake-oscillator model of Tamura. The second approach consists in wind tunnel tests on an aeroelastic model. The tests have been performed in uniform and turbulent wind on a rectilinear or curved model to quantify the effects of the curvature. These tests and the comparison to the theoretical models of VIV were carried out a posteriori as part of the master's thesis of the first author [4].

Both approaches are then compared and analyzed. With the vibration amplitude predicted by models, the arc is not able to maintain its structural integrity neither in terms of structural resistance nor fatigue. To reduce these vibrations and the high sensitivity of the arc to VIV, the main arc is equipped with a tuned mass damper, with a mass of 1500 kg (1.07% of the mass of the arc), placed at its top. Provided by the GERB company, the damper is a pendulum with two circular discs immersed in a cylindrical tank filled with silicon oil to damp the motion in both horizontal directions.

The damper is thus essential to limit the amplitude of vibrations under vortex induced vibrations. We face here a stability problem whereas most of the time, vibration is a comfort issue, like for footbridges. A monitoring system [3], coupled with meteorological wind data, continuously records the vibrations of the arc at the top and transmits alerts in the event of a malfunctioning of the TMD.

2. Description of the structure

Designed by Bureau Greisch, the “Arc Majeur” is made up of curved metal boxes with a square section of width b = 2.25 m. The grade of steel used is S355 J0 or J2 with a Corten treatment, like most of Bernar Venet's works (see Figure 1 and Figure 5). The small arc is made in one piece, with 20 mm thick plates while the main arc is made of 3 sections of respectively 20 mm, 30 mm and 40 mm thick plates, from top to bottom.

The main arc is divided into three sections for the transport and the erection. The parts are temporarily bolted together and then welded to ensure full section connection. The curvature radius is 38.5 m for an angular opening of 205°.

2.1. Dynamic properties of the main arc

The eigen modes and associated frequencies (f_0) are calculated using both a beam model and shell model. Indeed, the main arc does not have any inner diaphragm except for small transverse plates at 1/3 and 2/3 of the height to facilitate the joining of the elements during erection. The beam model does not consider the distortion of the cross section under torsion and overestimates the stiffness. Both models are rigidly connected at soil level (no foundations flexibility considered). Table 1 compares the calculated frequencies with those measured on site. Figure 2 depicts the shapes of first mode "out-of-plane" and second mode "in-plane". The beam model overestimates the frequencies by about 15% and the plate model is close to the measurements.

Table 1. Structure frequencies f_0

	Beam model	Shell model	Field measurements
Out-of-plane	0.94 Hz	0.78 Hz	0.81 Hz
In-plane	1.01 Hz	0.85 Hz	0.86 Hz

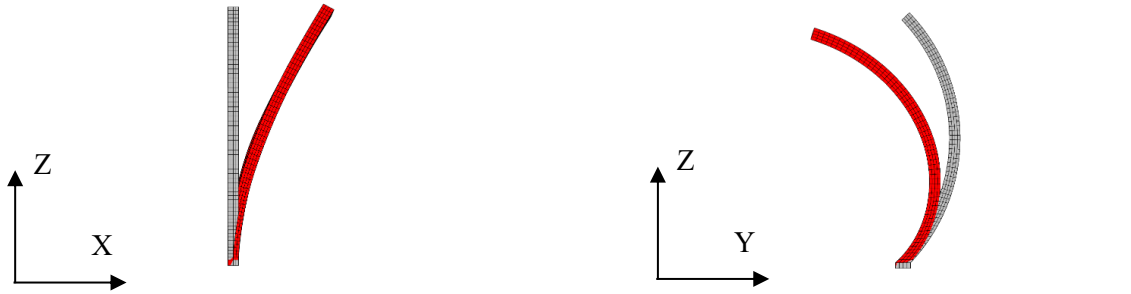

a) 1st eigen mode: out-of-plane vibration b) 2nd eigen mode: in-plane vibration

Figure 2. Vibration eigen modes of the main arc

2.2. Tuned mass damper

To reduce the vibrations due to wind, a tuned mass damper is placed at the top of the main arc to increase the damping minimal value up to 3%.

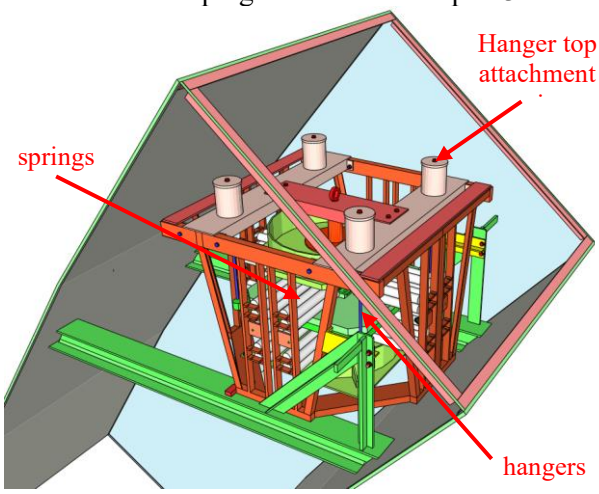

Figure 3. Tuned mass damper sketch

Figure 4. Tuned mass damper

The tuned mass damper (Figure 3 and Figure 4) is a 75 cm long pendulum (blue hangers, Figure 3). It consists of a 1500 kg moving mass made of two steel plates (in light green, Figure 3). To fine-tune

its natural frequency, the moving mass is connected to the fixed chassis using prestressed springs (horizontal light grey cylinders, Figure 3) on all four sides. The number of springs can vary from 4 to 16 per face depending on the desired optimum frequency. The damping forces are provided by two steel discs immersed in a silicon oil bath contained in two cylindrical tanks (in light green). The lower disk is linked to the moving mass and moves in the fixed lower tank. While the upper disk is fixed and bathes in the upper tank which is related to the moving mass.

After placing the damper, the measured equivalent damping ratios are 3.6% for the out-of-plane mode and 4.2% for the in-plane mode.

Moreover, aeroelastic properties of the arc for in-plane response are given in Table 2: the structural damping, the numbers of Strouhal, Scruton and Skop-Griffin and the mass ratio. To give an idea, according to experience, a Scruton number of 20 is the minimum to expect the structure to be safe.

Table 2. In-plane aeroelastic properties

	Strouhal $S_t = \frac{f_0 . b}{V_{cr}}$	Damping ξ	mass ratio $M = \frac{m_s}{m_{air}}$	Scruton $S_c = \frac{4.\pi.\xi.m_e}{\rho_{air}.b^2}$	Skop-Griffin $SG = 2.\pi.S_t^2.\ S_c$
Without TMD	0.12	0.32 %	332	10.3	0.93
With TMD	0.12	4.20 %	332	134.8	12.20

The equivalent mass, m_e, for the first in plane mode is equal to 1617 kg/m. It depends on the first mode shape and the mass distribution. It is not equal to the lineic mass as this later is not constant along the structure.

3. Wind Load according to the Eurocode

For the design of the Arch, the design office had to define the wind properties and loads. The next assumptions were adopted.

Figure 5. The "Arc Majeur" surroundings

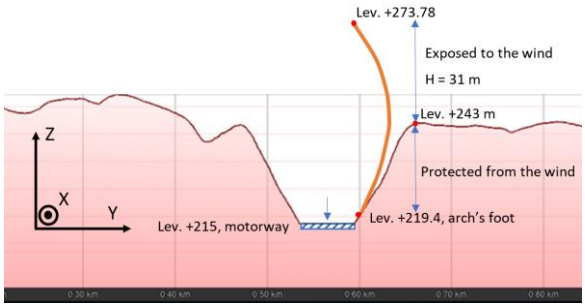

Figure 6. Arc in-plane cross section

Wind speeds and pressures are estimated according to Eurocode 1991-1-4 [1]. The reference wind speed $v_{b.0}$ is 23 m/s. The wind profiles are very different in the YZ plane (across the motorway) or XZ plane (in the direction of the motorway) due to the topology of the terrain (Figure 5).

In the latter case, the wind is parallel to the motorway and encounters almost no obstacles, so a category of terrain II is adopted with an average wind speed at the top of 30.9 m/s for a height of 60 m.

In the former case (in-plane wind), the situation is quite different. In this direction, topology and trees are present on both sides of the motorway and a category of terrain III is therefore adopted. Figure 6 represents a slice cut in the field for this direction. We can see that the arc is in a ditch that

protects it from the wind on its lower part. We adopt a height of 31 m for the top and the average wind speed is 23.4 m/s. The wind characteristics are summarized in Table 3.

Table 3. Wind characteristics

	Category	$V_{m,top}$ [m/s]	I_u [-]	$\frac{V_{m,10m}}{V_{m,top}}$ [-]
Out-of-plane	II	30.9	0.14	0.76
In-plane	III	23.4	0.22	0.75

4. Wind tunnel tests description

Aeroelastic tests are performed in the wind tunnel facility of the University of Liège. This one is a subsonic wind tunnel (Mach < 0.15). It includes a test section for aeronautical and automotive applications and a second test section for wind civil engineering applications. More information on this facility is available on the University of Liege website [5].

Tests are performed in uniform wind conditions and ignore the development of a boundary layer which is uncertain due to the complex topography of the site. This assumption is deemed to be safe concerning VIV. The purpose of the tests is to evaluate the vibration amplitude and the lock-in range for different Scruton numbers. The tests focus on a wind in the direction X of the motorway. So, the VIV concerns the in-plane mode of the arc. The effect of turbulence is tested in this configuration. The influence of the curvature is also evaluated by testing a straight model. Then for the curved model, its orientation is changed. So, wind is applied in Y and -Y direction to investigate this effect due to curvature.

4.1. The aeroelastic models

Two aeroelastic models are designed. The first is a true replica of the Arc Majeur. The second one is straight with the same developed length to investigate the effect of the curvature. The Figure 7 a) and b) show both models in test position. They are made of a hollow aluminium tube core and 3D printed plastic outer volumes.

a) Curved aeroelastic model b) Straight aeroelastic model

Figure 7. Models in test position in wind tunnel facility

The following similitudes are respected for aeroelastic tests. The geometrical similitude leads to a scale of 1/50 due to the wind tunnel dimensions. The side of square section is adapted thanks to the external plastic volumes to 2.25/50 = 0.045 m.

The mass ratio similitude is respected by imposing a lineic mass scale of $(1/50)^2$ to the model. This one is adjusted through the internal embossing of the 3D printing process. Moreover, the aluminium material for the core is necessary to obtain a so light model.

The critical velocity of VIV is imposed to be around 5 m/s to cover it precisely in the wind tunnel.

By consequence, the Strouhal similitude is achieved by setting the model in plane frequency to $f = S_t \cdot V_{cr}/b|_{model} = 0.12 \times 5 / 0.045 = 13.33$ Hz. This is done by correctly selecting the aluminium core cross-section based on the vibration theory of a cantilever beam. The external volumes are cut every 5 cm. So, they add mass to the model and its shape but no stiffness. After measurement, the first in-plane frequency is 13.00 Hz, close from 13.33 Hz.

Finally, the respect of the Scruton similitude leads to a critical damping ratio equal to 0.23%. It is different from the one of the prototype (0.32%), because the equivalent mass of the model is lower than the prototype one. The measured mean damping ratio of the model is 0.07%. The multiple logarithmic decrement method is used and is compared to different approaches. This is detailed in the master thesis [4]. The damping ratio is increased by adding adhesive bands to the model to dissipate energy. This method allows to cover a damping range from 0.07 to 0.44% and to test the model with a Scruton number close to the prototype one.

4.2. Experimental setup and test procedure

The experimental setup consists of a triaxial wireless accelerometer placed at the top of the model and an anemometer to record the incoming wind speed.

Turbulence is measured using a cobra probe. Two different turbulence configurations are tested: a low turbulent wind and a turbulent one generated with a turbulent grid. The mean results in terms of turbulence intensity I_u and dimensionless turbulence scale L_u^*/b of the wind are presented in Table 4. As usual, the dimensionless turbulence scale is lower than the one advised by the EN1991-1-4 annex B [1]. For a category of terrain II, at a height of 60 m, the later is $L_u^*/b = 160/2.25 = 71.1$. This difference increases for the turbulent wind. This is why the turbulent results should be taken with caution when scaled up to the prototype.

Table 4. Wind tunnel turbulence characteristics

	I_u	L_u^*/b
Low turbulent	0.4 %	7.8
Turbulent	4.9 %	3.3

The following test procedure is repeated for each configuration of test defined by the wind turbulence (low or high), the structural damping and the orientation of the model.

First, five wind off free decays are performed to measure the across wind frequency and structural damping. At test scale, the VIV critical wind speed is expected to be around 5 m/s. So, the wind velocity is increased from 3 m/s to the end of the VIV curve with steps of 0.8 or 0.4 m/s if necessary. When the response of the model becomes stationary, a 60 seconds acceleration measurement is performed. It corresponds to 15 minutes at the prototype time scale to achieve the same number of cycles thanks to the frequencies ratio.

For each configuration, the wind velocity is recorded, and the amplitude of vibration is evaluated. The Power Spectral Density (PSD) of the signal is computed to analyse its frequency content.

5. Vortex induced vibrations

The critical wind speeds (V_{cr}) for the VIV are 15.2 m/s for a wind perpendicular to the motorway (Y direction) and 16.1 m/s for a wind parallel to the motorway (X direction). These speeds are lower than the average wind speed observed in Lavaux-Saint-Anne and there is therefore a risk of VIV, according to EN1991-1-4 [1].

The amplitudes of vibration are calculated according to several approaches and the results of the wind tunnel tests. They must be compared to the maximum admissible displacements at the top of the arc, that are respectively 66 cm, 44 cm and 34 cm at ULS, SLS and fatigue state. It is the fatigue verification which is the most limiting factor on the VIV amplitude.

5.1. Eurocode approach

The amplitudes of the vibrations (Y_F) are calculated according to the method 2 of Eurocode 1991-1-4 [1] and its national Belgian annex [2] for a critical damping ratio (ξ) of 0.3% corresponding to steel chimney. The results are given in Table 5. This table also gives the number of cycles (N), within 50 years, for each frequency according to Hansen's formula [2] for the fatigue verifications.

Table 5. VIV amplitudes according to the Eurocode [1, 2]

	V_{cr} [m/s]	Y_F $\xi = 0.3\%$ [m]	Y_F $\xi = 3.0\%$ [m]	C_C [-]	$K_{a,max}$ [-]	a_L [-]	k_p [-]	σ_y [m]	N [-]
Out-of-plane	15.2	1.07	0.29	0.076	6.0	0.4	4.06	0.07	32 950
In-plane	16.1	1.15	0.32	0.074	6.0	0.4	3.96	0.08	1 330 000

5.2. Wind tunnel results

The results are presented as non-dimensional values and so can either be extended to the prototype scale or to the model one.

5.2.1. Reference test. The reference test is the curved model in a low turbulent flow. The test is performed for five different Scruton numbers. The VIV response curves are presented in Figure 8 a) in terms of relative amplitude Y_F/b function of the reduced velocity $V_r = V/(f_0.b)$. The Figure 8 b) shows the PSDs of the acceleration signals for Sc = 3.0 and this for all the points of the blue curve of Figure 8 a). This minimal value of Sc = 3 is chosen for the Figure 8 b) because it is the one for which the lock-in range appears best. In the two figures, the lock-in range extends from V_r = 8 to 20, for Sc = 3. It corresponds to the high vibration amplitude in Figure 8 a). In Figure 8 b), this range corresponds to the PSDs for which the peaks of the vortex shedding frequency f_{vs} appear at f_0 and don't appear at the expected value predicted by the Strouhal law: $f_{vs} = S_t.f_0.V_r$. In this range, the peaks are concentrated at f_0 as vortex shedding frequency is imposed by the structure. Above V_r = 20, the model restarts to vibrate at the different frequencies f_{vs}, f_0 and $f \approx 5\ f_0$, corresponding to its second modal frequency.

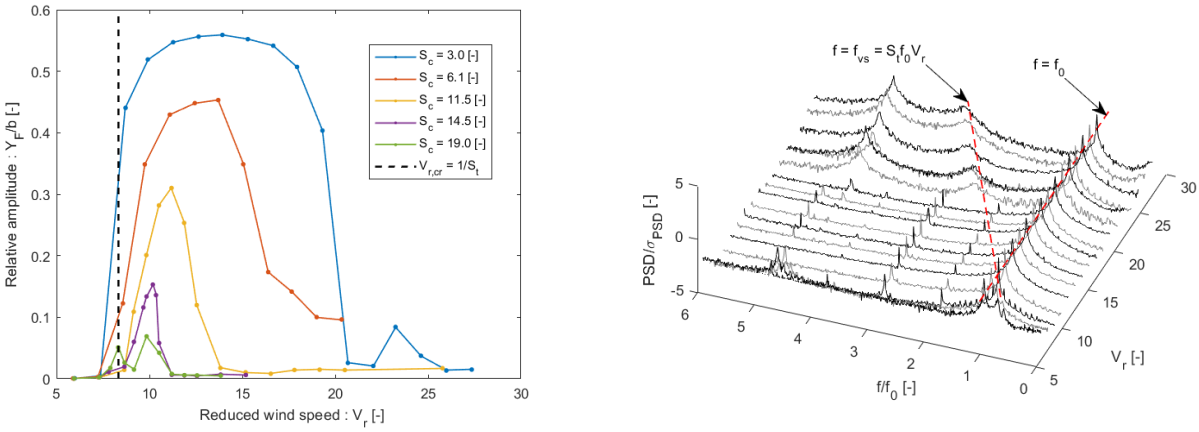

a) VIV response for different Scruton b) Lock-in range: PSD for Scruton = 3.0

Figure 8. Curved model in a low turbulent flow

These results are summarized in terms of maximum relative amplitude and lock-in range function of Scruton number, in Figure 9 by the blue curves.

5.2.2. Curvature and wind turbulence effects. Through the test of the straight model, the effects of curvature are analysed for the same flow conditions, for five different damping. The results are

summarized in red in the Figure 9. There is no major difference between the curved and the straight model in terms of amplitude and lock-in range. Nevertheless, in the acceleration measurements, it appears that the straight model vibrates also in the along wind direction. This is caused by the dynamic interaction due to closely spaced modal frequencies in the two vertical planes of vibration. More details, such as time histories of acceleration and full VIV response curves are available in the master thesis [4].

The curved model is also tested in turbulent flow conditions. It shows the drastic effect of turbulence on the mitigation of the VIV response. A wind turbulence intensity of only 4.9% disrupts totally the vortex shedding and so the resonance ability of the phenomenon. This intensity is low compared to $I_u = 14\%$ from Table 3. Those results are presented in yellow in Figure 9.

Finally, by crossing the blue curve with the Scruton number of the "Arc Majeur" without TMD ($S_c = 10.3$), the Figure 9 allows to predict a vibration amplitude of $Y_F = 0.34$ b = 0.77 m and a lock-in range going from $V_r = 8.3\ to\ 13.4$. It corresponds to $V = V_r . f_0 . b = 16$ to 26 m/s.

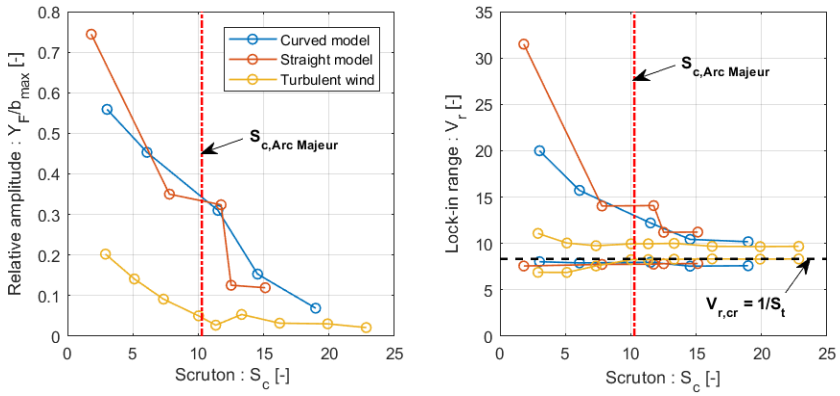

Figure 9. Comparison of relative amplitude and lock-in range vs. Scruton number

5.2.3. Wind direction effects. The effect of the wind direction is studied disregarding the topography influence. It focuses on the 3D effects of arc's curvature on the wind flow. The experimental points are not presented in this paper. Only the main conclusions are drawn. For a wind V_y, in the direction of the Y axis (Figure 2), the VIV response is reduced compared to the X direction, V_x, tested previously for all Scruton range tested. For a wind in the opposite direction -V_y, the response is amplified of about 20% for very low Scruton (around 3.5) and is decreased for higher ones. Tests for 45° orientations show amplitudes 10 times lower.

5.2.4. Comparison to other tests and to Skop-Griffin curve. For validation, the present experimental results are compared, in logarithmic scale, in Figure 10, to others references from the literature performed on rigid straight cylinders [5] and to the experimental Skop-Griffin curve [7] given by:

$$\frac{Y_F}{b} = \frac{1.29}{[1 + 0.43\ SG]^{3.35}}$$

The experimental points corresponding to a low wind turbulence show the same trend but are in the lower range of amplitude. This is maybe because of the intrinsic difference between the constant mode shape of rigid cylinders and the mode of a cantilever beam. The points with a higher turbulent wind intensity clearly stand out with a lower amplitude.

5.3. Mathematical modelling of VIV

Figure 11 shows the predicted amplitudes of the mathematical models as a function of the Scruton number and covers the range of Scruton of the "Arc Majeur" with and without TMD.

5.3.1. Eurocode models [1] [2]. The full curves of the normative model 2 of the Eurocode and the model 1 are plotted in Figure 11.

5.3.2. Harmonic model [8]. A harmonic forcing model of VIV is implemented, with a correlation length of the excitation integrated on the first mode. This one appears to be close from the model 1 of the Eurocode. As they are deduced form linear dynamics, they are both unbounded for zero damping and do not follow the experimental curves.

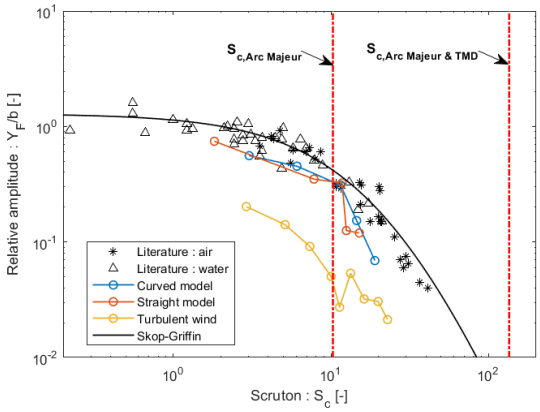

Figure 10. Comparison to literature tests and Skop-Griffin curve (Experimental data: circles)

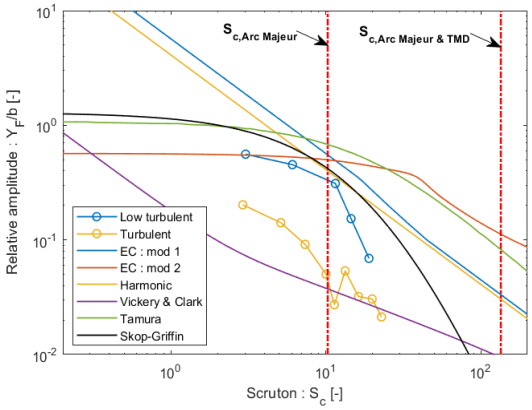

Figure 11. Comparison to mathematical models (Experimental data: circles)

5.3.3. Spectral model of Vickery and Clark [9]. As they propose a spectral power density to represent the vortex shedding, the excitation is more spread in frequency and is unable to represent the self-exciting regime and so is out of scope for this study. As it is also linear dynamics, the response is unbounded for zero damping. Nevertheless, because of this spreading of frequencies, this model appears to be more in accordance with tests in turbulent flow.

5.3.4. Wake-oscillator model of Tamura [10]. The implementation of Tamura's model by Rigo [10] is used. It is based on non-linear dynamics to represent the excitation, the wake. It enables to represent a bounded response for zero damping, thanks to a limit cycle. Its allure is similar to the Eurocode model 2.

The latter two models are the more physical to cover the full Scruton range with the transition zone between both regimes, self-exciting and forcing regime. But the transition zone appears at too high Scruton compared to the experimental tests and the Skop-Griffin curve.

6. Fatigue resistance

Table 5 gives the amplitude vibration (according to EN 1991-1-4) and the number of cycles for each wind direction or mode shape vibrations. Stresses range variations at critical points are then deduced and compared to the S-N curves given by the Eurocode EN 1993-1-9. According to the wind rose of Florennes (Figure 13), the main winds come from the Southwest (along Y axis) and results in 2/3 of the cycles for the out-of-plane mode (mode 1) and 1/3 for the in-plane mode (mode 2). According to Miner's rule, damages for each wind direction are cumulated. Figure 12 displays the fatigue lifetime as a function of the damping ratio with the amplitudes according to the forensic verifications (Eurocode) or with the amplitudes recorded during the wind tunnel tests (low I_u). For low damping ratios, tests results are in good agreement with the Eurocode predictions, but the fatigue safety increases more rapidly with the damping ratio for the tests results than the code. This can be explained by Figure 11 where we can observe that the transition zone which corresponds to the rapid drop in vibration amplitudes occurs for much lower Scruton numbers with the test results than with the Eurocode method 2. The drop is also much more rapid.

Based on the Eurocode, a minimum critical damping ratio of 3.0% is finally retained. With the use of the TMD, the vibration amplitudes are reduced by a factor of 3.

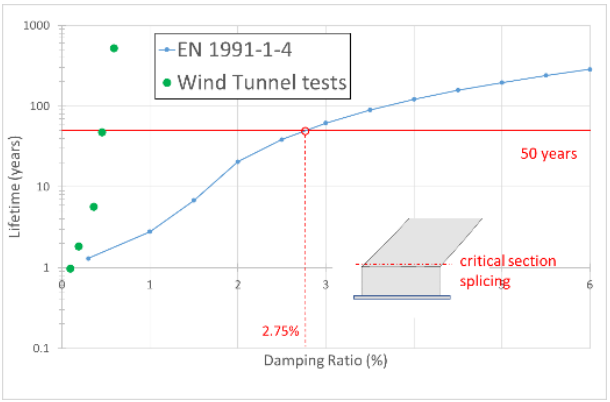

Figure 12. Lifetime vs. critical damping ratio (ξ)

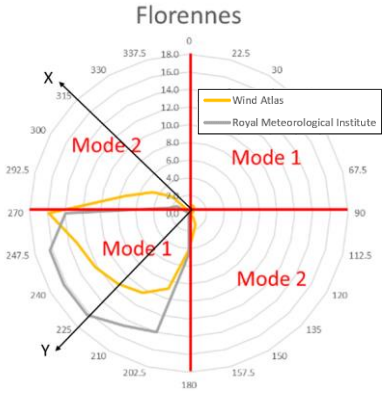

Figure 13. Florennes wind rose for VIV critical wind speeds range

7. Conclusions

The "Arc Majeur" is a 60-meters-tall structure which has a square section of 2.25 m side. From a first aspect, its behaviour sounds simple but because of its large slenderness and low stiffness, it is sensitive to the vibrations induced by Von Karman's vortices. Under these vibrations, the resulting movements are too large to ensure its long-term stability. A tuned mass damper was therefore placed at its top to limit the motion.

Firstly, the arc has been designed according to the recommendations of the Eurocode 1991-1-4.

Then, aeroelastic tests revealed that the transition zone between self-exciting response (at hight amplitude) and forcing one appears at too high Scruton number in the Eurocode model 2. The Skop-Griffin approach seems to give the best correspondence with the experimental results.

Finally, according to the wind tunnel tests, it appears that the structural damping provided by the TMD is sufficient and could be less to still ensure the safety of the structure.

References

[1] Eurocode 1991-1-4 April 2005: Actions on structures- Part 1-4: General actions – Wind actions.A reference

[2] NBN 1991-1-4 ANB:2010 (F). Eurocode 1: Actions on structures - Part 1-4: General actions – Wind actions. National annex.

[3] Duchêne Y, Seret S, de Ville de Goyet V, Ligot J, Verstraelen E, Philippart A, The Arc Majeur, when art challenges technology, 2021, IABSE Congress Ghent - Structural Engineering for Future Societal Needs.

[4] Palm A, Analyse dynamique de l'Arc Majeur sous l'effet de détachement de tourbillions de Von Karman, 2022, Master Thesis, Université de Liège - Faculté des Sciences Appliquées

[5] ULiège, The University of Liège Wind Tunnel Facility: Technical description, 2009, https://www.wind-tunnel.uliege.be.

[6] Facchinetti M L, De Langre E et Biolley F, Coupling of structure and wake oscillators in vortex-induced vibrations, 2003, Journal of fluids and structures, p. 12.

[7] Hémon P, Vibrations des structures couplées avec le vent, 2006, Les éditions de l'école polytechnique, p. 76.

[8] Wertz F, Modelling of the response of a slender structure to vortex shedding in the atmospheric boundary layer, 2015, Master Thesis, Université de Liège- Faculté des Sciences Appliquées.

[9] Vickery BJ et Clark AW "Lift or across-wind response of tapered stacks". In : Journal of the structural division (1972), p. 1-21.

[10] Rigo F, Andrianne T et Denoël V "Parameter identification of wake-oscillator from wind tunnel data". In : Journal of Fluids and Structures (2022), p. 2-9.